

Appendix S1. Pika occupancy survey methods.

Pika occupancy records at each study site were collected using two approaches. First, we conducted annual pika occupancy surveys from 2010 to 2012 (Jeffress *et al.*, 2012). In each park, survey locations were selected at random using the Generalized Random Tessellation-Stratified algorithm (GRTS; Stevens and Olsen, 2004), which provided a spatially balanced sample of survey sites across previously mapped pika habitat (e.g., talus fields and lava beds). Each individual survey site consisted of a 12 m radius plot centrally located on the random point identified by the GRTS. Within this plot, we systematically searched for evidence of current pika occupancy (e.g., fresh scat, fresh hay pile, vocalization, visual confirmation) to determine pika presence or absence. To standardize results between sites and across years, personnel were provided thorough group training for survey protocols and accurate aging of pika sign. Because of their territorial vocalizations, hay piling activity and use of latrine sites, pika detection probabilities exceed 90% (Beever *et al.*, 2010; Erb *et al.*, 2011; Jeffress *et al.*, 2011), thus we have a high level of confidence that our occupancy surveys accurately reflect the presence/absence patterns of the species at each study area. Site accessibility varied based on climatic conditions at each park; we surveyed each site annually during the snow free period, which ranged between late June and early November, depending on study site. The resulting data provided georeferenced point locations for both presence and absence of pikas.

Second, in addition to occupancy surveys we included presence-only records collected in each park during scat sampling for genetic analysis (Castillo *et al.*, in prep). Survey areas were selected non-randomly, targeting regions for which little to no genetic data were available. In each region, one or more habitat patches was searched exhaustively for fresh pika scat, and a georeferenced point location was recorded at each site where fresh scat was collected. Sites were spaced >50 m apart to avoid sampling the same individual multiple times. Locations were also recorded where scat was observed when traversing between surveyed patches. The resulting data provided georeferenced point locations for pika presence only.

Uneven sampling across an area can introduce bias into species distribution models, although this issue is more problematic for presence-only versus presence-absence datasets (Phillips *et al.*, 2009). To avoid this issue when combining the two datasets, we removed genetic locations which were within 100 m of occupancy survey sites. For both data sources combined, the total number of presence and absence records per park ranged from 121 to 329 (Table 1, main manuscript).

References (Appendix S1)

- Beever EA, Ray C, Mote PW, Wilkening JL (2010) Testing alternative models of climate-mediated extirpations. *Ecological Applications*, 20, 164-178.
- Castillo JA, Epps CW, Jeffress M, *et al.* In prep. Landscape configuration and climate shape functional connectivity for a climate-sensitive species, the American pika (*Ochotona princeps*).
- Erb LP, Ray C, Guralnick R (2011) On the generality of a climate-mediated shift in the distribution of the American pika (*Ochotona princeps*). *Ecology*, 92, 1730-1735.
- Jeffress MR, Apel J, Garrett LK, *et al.* (2011) Monitoring the American pika (*Ochotona princeps*) in the Pacific West Region-Crater Lake National Park, Craters of the Moon National Monument and Preserve, Lassen Volcanic National Park, and Lava Beds

National Monument: Narrative Version 1.0. Natural Resource Report NPS/UCBN/NRR-2011/336. National Park Service, Fort Collins, Colorado, USA.

Phillips SJ, Dudik M, Elith J, *et al.* (2009) Sample selection bias and presence-only distribution models: implications for back-ground and pseudo-absence data. *Ecological Applications*, 19, 181-197.

Stevens DL, Olsen AR (2004) Spatially balanced sampling of natural resources. *Journal of the American Statistical Association*, 99, 262-278.

Table S1. Information for genetic samples for each park. The first row shows each park's 4-letter identification code, while the second row shows the number of individuals samples in each park. The third row shows expected and observed heterozygosity (H_e/H_o , respectively), and the final rows show the number of alleles observed per locus for each study site.

Park Name	CRLA	CRMO	GRSA	GRTE	LABE	LAVO	ROMO	YELL
Individuals	122	60	54	194	51	125	221	26
H_e/H_o	0.46/0.51	0.51/0.58	0.62/0.73	0.63/0.69	0.57/0.64	0.56/0.65	0.58/0.77	0.64/0.74
OCC03	8	1	6	10	3	8	14	7
OCC04	6	7	8	11	6	9	14	13
OCP03	2	2	7	2	7	5	9	2
OCP04	7	7	9	8	6	8	9	8
OCP07	7	6	10	11	7	9	13	8
OCP20	9	3	6	14	6	8	10	7
OCC09	4	5	3	8	7	6	5	8
OPC01	2	5	6	6	4	5	22	8
OCP02	7	9	6	10	5	6	9	7
OCP08	4	6	16	13	11	11	15	13
OCP14	6	5	5	5	7	3	5	6
OCC02	2	5	5	8	3	2	5	5
OCP05	6	8	6	9	7	6	8	7
OCP12	8	6	6	13	6	9	10	7
OCP17	2	3	8	2	3	6	5	3
OCP18	3	3	6	8	4	5	8	6
OCP27	3	7	11	11	6	9	12	13
OCP06	5	5	13	15	6	7	12	14
OCP09	14	14	14	20	5	8	21	9
OCP11	5	3	6	7	5	7	8	7
OCP16	2	4	6	7	6	6	8	7
OCP24	5	6	5	7	3	7	8	5

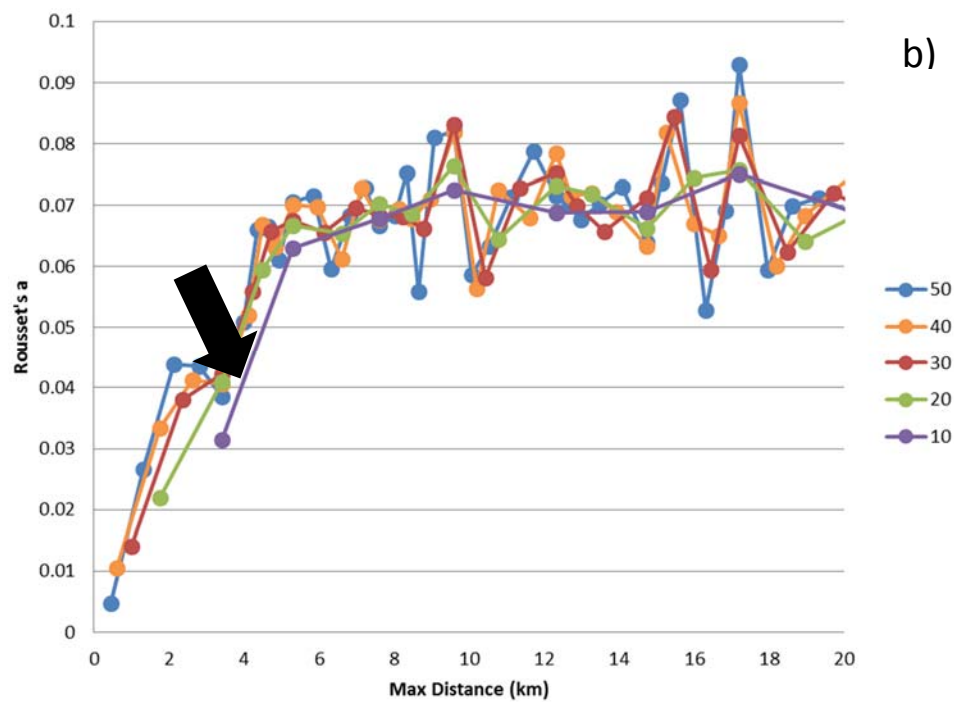
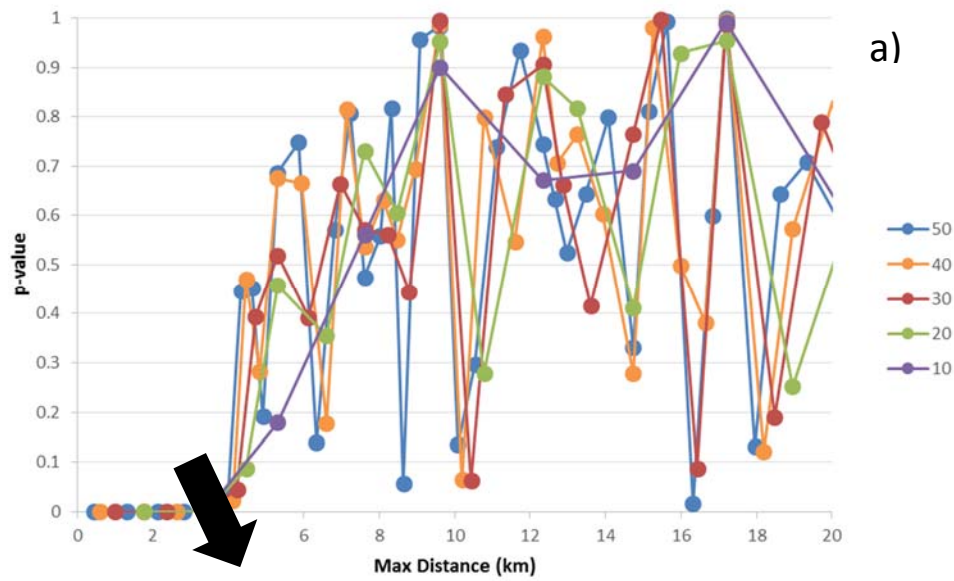
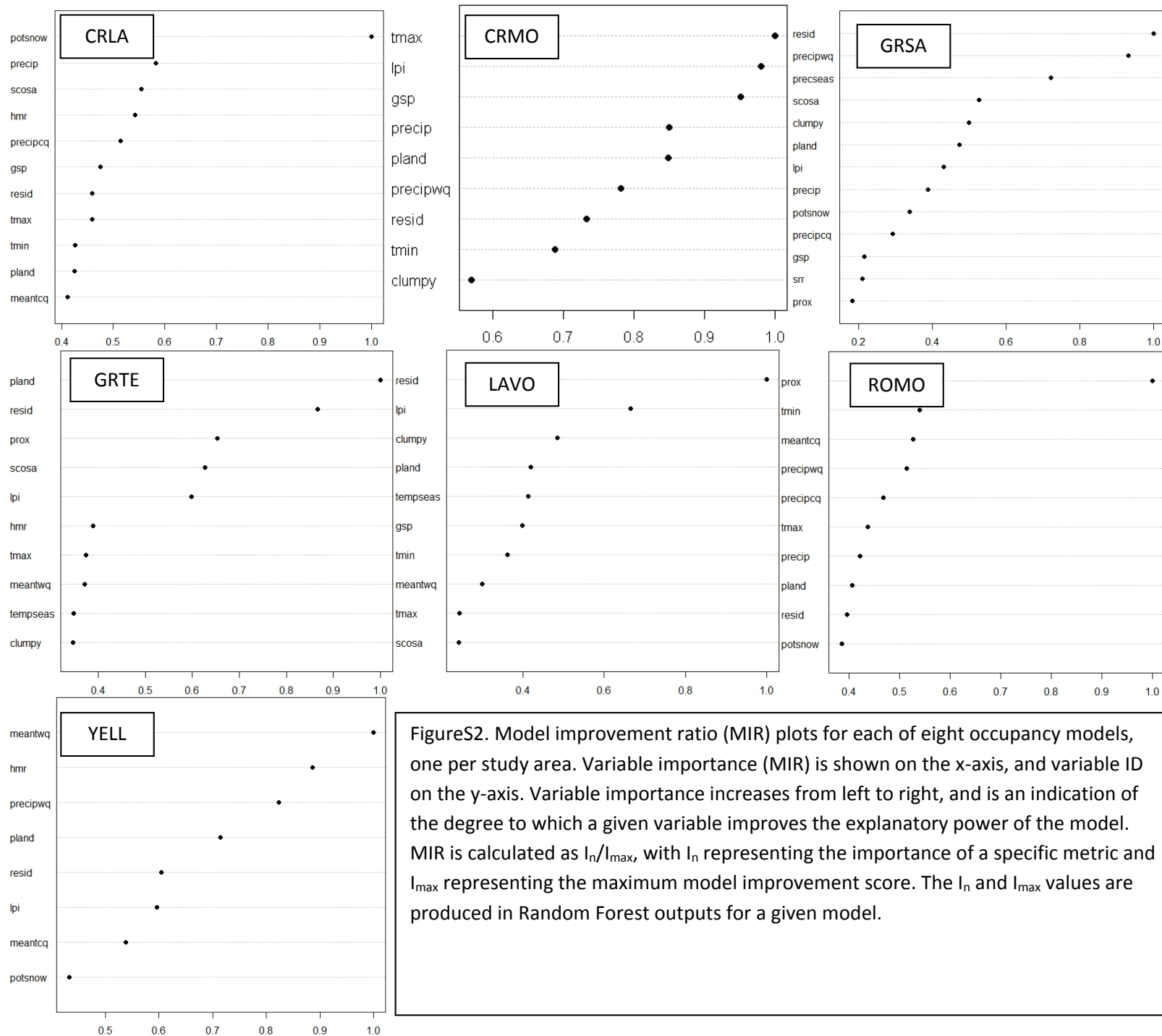
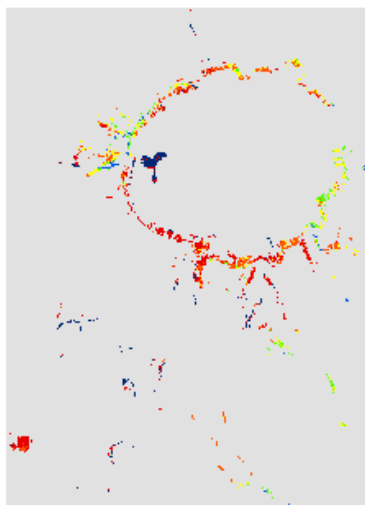


Figure S1. Examples of Mantel correlogram approach for estimating genetic neighborhood size, from Grand Teton National Park (GRTE). The correlation between genetic distance and Euclidean distance (a) is no longer significant after ~4.3 km (black arrow). This also corresponds to a large increase in genetic distance (b, Rousset's a , black arrow).

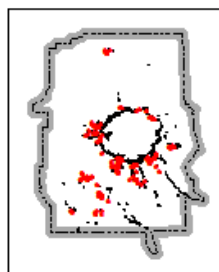


FigureS2. Model improvement ratio (MIR) plots for each of eight occupancy models, one per study area. Variable importance (MIR) is shown on the x-axis, and variable ID on the y-axis. Variable importance increases from left to right, and is an indication of the degree to which a given variable improves the explanatory power of the model. MIR is calculated as I_n/I_{max} , with I_n representing the importance of a specific metric and I_{max} representing the maximum model improvement score. The I_n and I_{max} values are produced in Random Forest outputs for a given model.

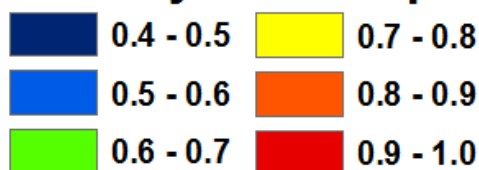
Current



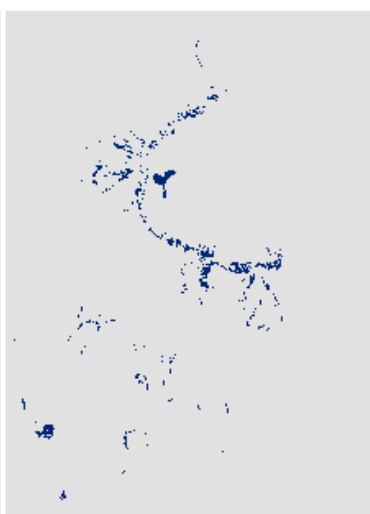
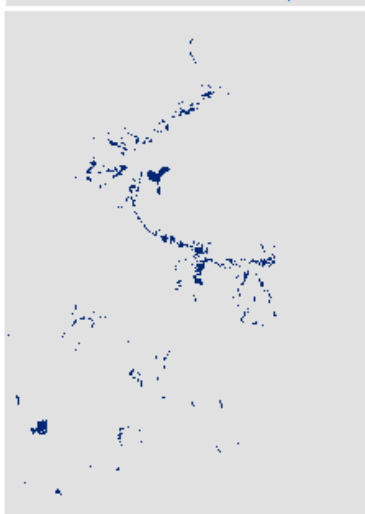
CRLA



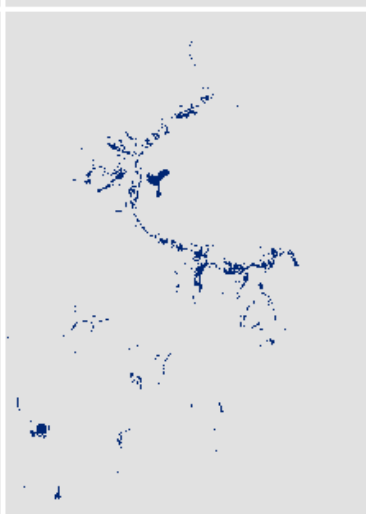
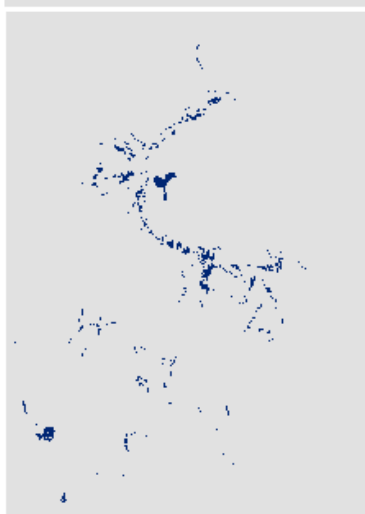
Probability of Occupancy



RCP 4.5



RCP 8.5



2011-2040

2041-2070

2071-2099

Figure S3. Predicted pika distributions in CRLA. The uppermost map shows predicted current probability of occupancy using contemporary climate and landscape variables, while the lower two rows of maps show predicted probability of occupancy using the ensemble climate model with two carbon forcing (RCP) scenarios and landscape variables. Individual sampling locations are shown in red in the upper right study area map.

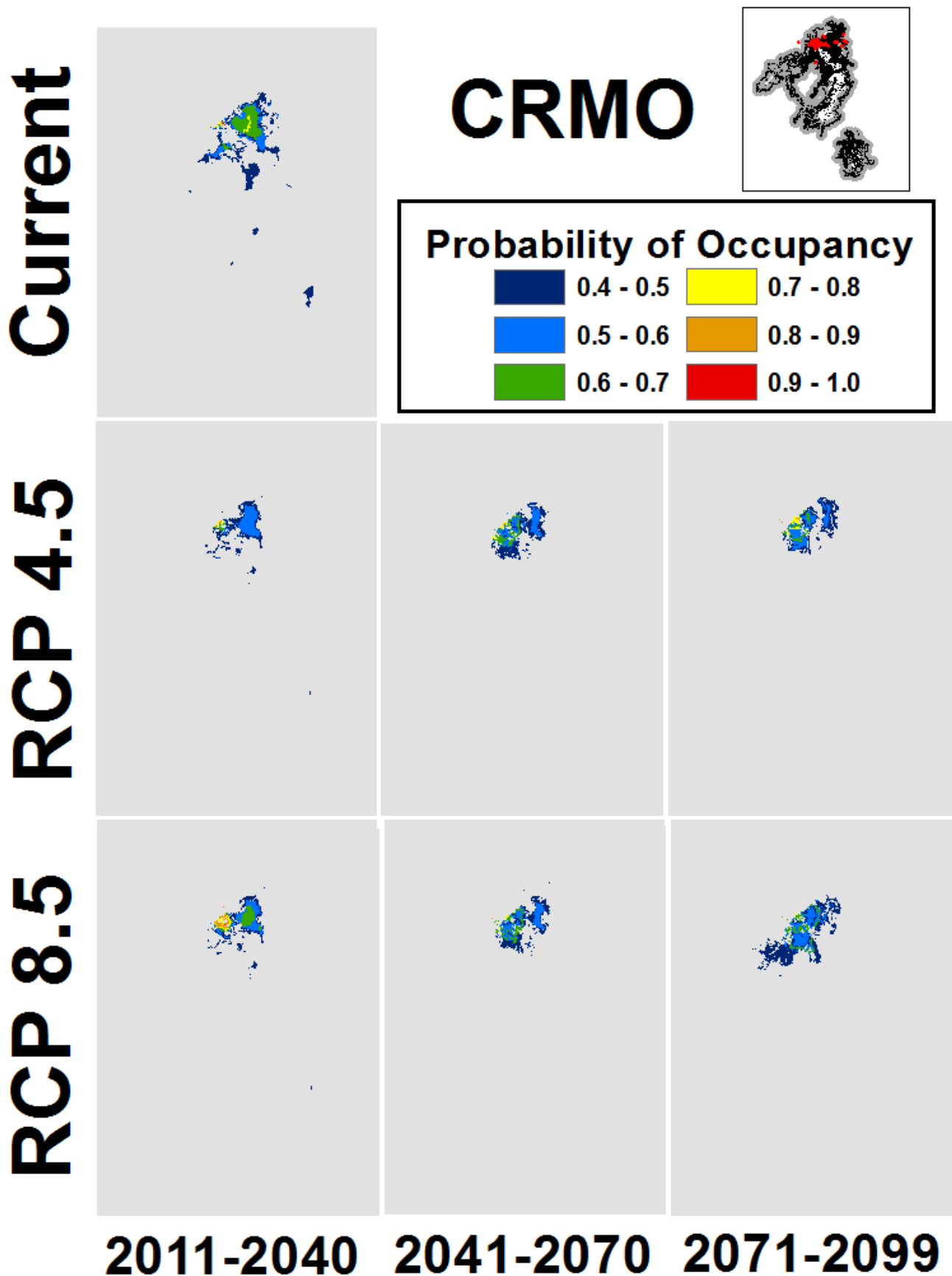


Figure S4. Predicted pika distributions in CRMO. The uppermost map shows predicted current probability of occupancy using contemporary climate and landscape variables, while the lower two rows of maps show predicted probability of occupancy using the ensemble climate model with two carbon forcing (RCP) scenarios and landscape variables. Individual sampling locations are shown in red in the upper right study area map.

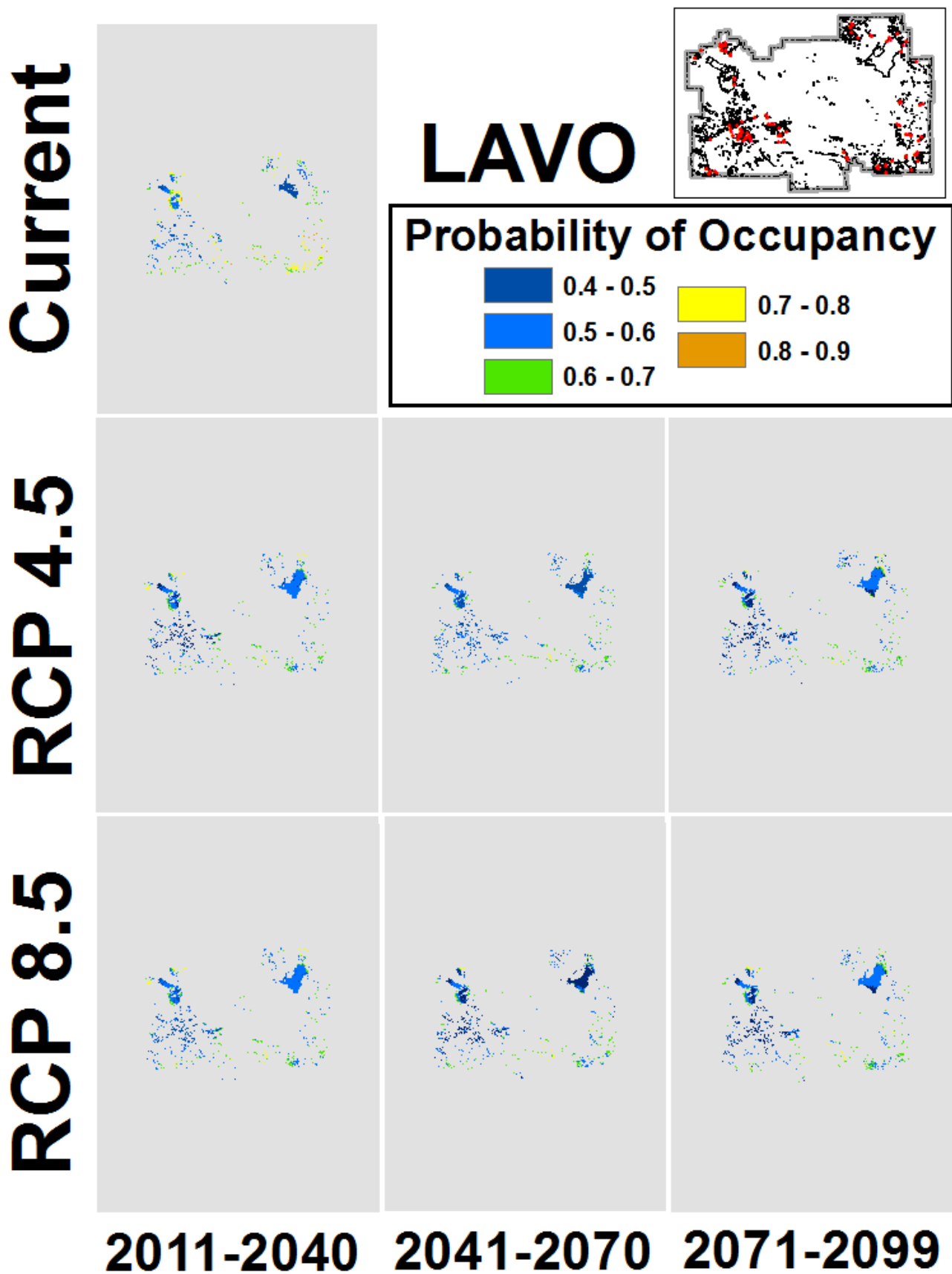


Figure S5. Predicted pika distributions in LAVO. The uppermost map shows predicted current probability of occupancy using contemporary climate and landscape variables, while the lower two rows of maps show predicted probability of occupancy using the ensemble climate model with two carbon forcing (RCP) scenarios and landscape variables. Individual sampling locations are shown in red in the upper right study area map.

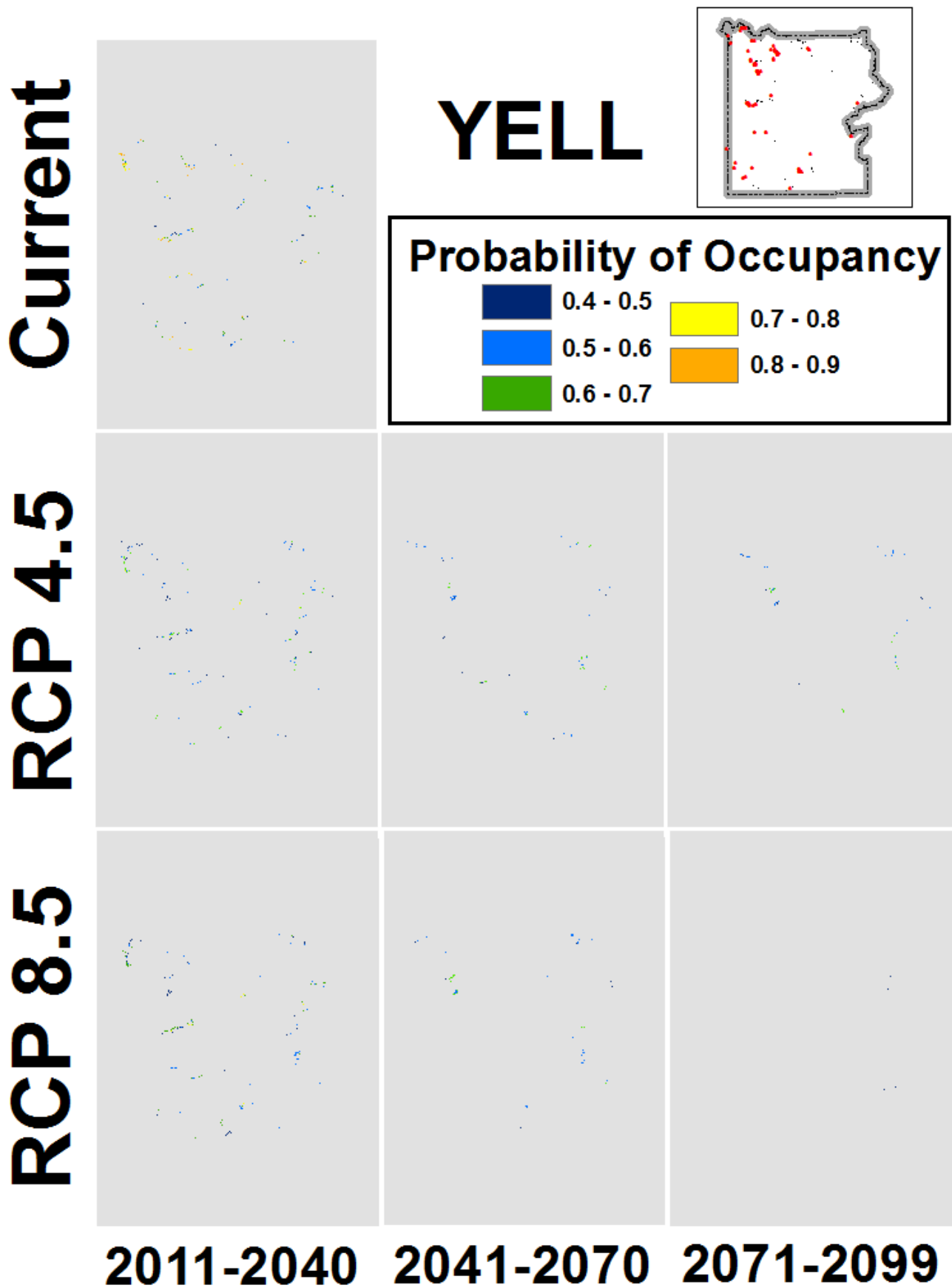


Figure S6. Predicted pika distributions in YELL. The uppermost map shows predicted current probability of occupancy using contemporary climate and landscape variables, while the lower two rows of maps show predicted probability of occupancy using the ensemble climate model with two carbon forcing (RCP) scenarios and landscape variables. Individual sampling locations are shown in red in the upper right study area map.